Automated Optic Disc Localization and Contour Detection Using Ellipse Fitting and Wavelet Transform

P.M.D.S. Pallawala[1], Wynne Hsu[1], Mong Li Lee[1], and Kah-Guan Au Eong[2,3]

[1] School of Computing, National University of Singapore, Singapore
{pererapa, whsu, leeml}@comp.nus.edu.sg,
[2] Ophthalmology and Visual Sciences, Alexandra Hospital, Singapore
[3] The Eye Institute, National Healthcare Group, Singapore
kah_guan_au_eong@alexhosp.com.sg

Abstract. Optic disc detection is important in the computer-aided analysis of retinal images. It is crucial for the precise identification of the macula to enable successful grading of macular pathology such as diabetic maculopathy. However, the extreme variation of intensity features within the optic disc and intensity variations close to the optic disc boundary presents a major obstacle in automated optic disc detection. The presence of blood vessels, crescents and peripapillary chorioretinal atrophy seen in myopic patients also increase the complexity of detection. Existing techniques have not addressed these difficult cases, and are neither adaptable nor sufficiently sensitive and specific for real-life application. This work presents a novel algorithm to detect the optic disc based on wavelet processing and ellipse fitting. We first employ Daubechies wavelet transform to approximate the optic disc region. Next, an abstract representation of the optic disc is obtained using an intensity-based template. This yields robust results in cases where the optic disc intensity is highly non-homogenous. Ellipse fitting algorithm is then utilized to detect the optic disc contour from this abstract representation. Additional wavelet processing is performed on the more complex cases to improve the contour detection rate. Experiments on 279 consecutive retinal images of diabetic patients indicate that this approach is able to achieve an accuracy of 94% for optic disc detection.

1 Introduction

Digital retinal images are widely used in the diagnosis and follow-up management of patients with eye disorders such as glaucoma, diabetic retinopathy, and age-related macular degeneration. Glaucoma is the second leading cause of blindness in the world, affecting some 67 to 105 million patients [20]. In glaucoma, an abnormally raised intraocular pressure damages the optic nerve and results in morphological changes in the optic disc. This leads to an increase in the size of the optic cup. Diabetic retinopathy is also a leading cause of blindness and visual impairment in many developed countries and accounts for 12,000 to 24,000 blind cases in United States alone every year [5].

T. Pajdla and J. Matas (Eds.): ECCV 2004, LNCS 3022, pp. 139–151, 2004.

The automated detection of optic disc has several potential clinical uses. First, the vertical diameters of the optic cup and disc may aid the diagnosis of glaucoma [3]. Changes in these parameters of the optic disc in serial images may indicate progression of the disease. Second, it allows the identification of the macula using the spatial relationship between the optic disc and macula. The macula is located on the temporal aspect of optic disc and is situated at a distance of about 2.5 disc diameters from the centre of the optic disc [9]. Occurrence of lesions in the macula region as a result of diabetic retinopathy and age-related macular degeneration are often sight-threatening. Identifying the macula allows highly sensitive algorithms to be designed to detect signs of abnormality in the macular region.

The optic disc appears as an elliptical region with high intensity in retinal images (see Fig. 1). The vertical and horizontal diameters of an optic disc are typically 1.82 ± .15mm and 1.74 ± .21 mm respectively [3]. Clinically, optic disc measurements can be obtained by approximating the disc to an ellipse [2].

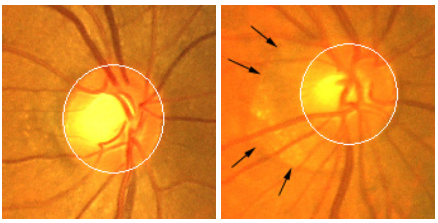

(a) (b)

Fig. 1. (a) Outline of optic disc (white ellipse), (b) Outline of optic disc with peripapillary chorioretinal atrophy (black arrows)

While existing algorithms [8,10,13,14,15,16,18] employ a variety of techniques to detect optic disc, they are neither sufficiently sensitive nor specific enough for clinical application. The main obstacle is the extreme variation of the optic disc intensity features and the presence of retinal blood vessels (Fig. 1(a)). Peripapillary chorioretinal atrophy which are commonly seen in myopic eyes also increase the complexity of optic disc detection. This presents as a bright crescent-shaped area adjacent to the optic disc, usually on its temporal side (Fig. 1(b)), or as a bright annular (doughnut-shaped) area surrounding the optic disc.

Our proposed approach overcomes the above challenges as follows. We first approximate the optic disc boundary via the use of Daubechies wavelet transform and intensity-based techniques. Next, an ellipse fitting algorithm is employed to detect the optic disc contour in the optic disc boundary region. Experiments on 279 consecutive retinal images disclosed that we were able to achieve an accuracy of 94% for optic disc detection and 93% accuracy based on mean vertical diameter assessment.

2 Related Work

There has been a long stream of research to automate optic disc detection. Techniques such as active contour models [10,16], template matching [8], pyramidal decomposition [8], variance image calculation [18] and clustering techniques [13] have been developed. Among them, active contour-based models have been shown to give better results compared to the other techniques. We evaluate active contour models on optic discs ranging from least contour variants to complex variations, and discuss their result and limitations here.

Snakes or active contours [7,11,17] are curves defined within an image domain that can move under the influence of internal forces coming from the curve itself and external forces computed from the image data. There are two types of active contour models: parametric active contours [22] and geometric active contours [23]. Parametric active contours synthesize parametric curves within image domains and allow them to move towards desired features, usually edges. A traditional snake is a curve X(s) = [x(s), y(s)], s ∈ [0, 1], that moves through the spatial domain of an image to minimize the energy functional

$$E = \int_0^1 \frac{1}{2}[\alpha|\dot{x}(s)|^2 + \beta|\ddot{x}(s)|^2] + \gamma E_{ext}(x(s))ds \tag{1}$$

where α, β, γ are weighting parameters that control the snake's tension, rigidity and influence of external force, respectively, and $\dot{x}(s)$ and $\ddot{x}(s)$ denote the first and second derivatives of x(s) with respect to s. The external energy function E_{ext} is derived from the image so that it takes on its smaller values at the features of interest, such as boundaries.

Analysis of the digital retinal images reveals that the use of the gradient image to derive the external energy function needed by the active contours model is not suitable because the gradient image contains too much noise arising from the retinal vessels. Even after removing retinal vessels [6] from the gradient image, it may not be complete and the removal process may introduce operator that will distort the original optic disc contour. Another option is to use intensity-based external force E_{ext} model. Here, we use the gray value of the green layer of the original image as the external force. Table 1 shows the results for various weight parameters. Note that the intensity-based external force model tends to produce poorer results. Further attempts to improve results using morphological operators have not been successful due to wide variations in optic disc features.

D.T. Morris et al. [16] reported the use of active contour models to detect the optic disc with a preprocessing step to overcome these problems. Images are first preprocessed using histogram equalization. This is followed by the use of pyramid edge detector. While this approach shows improved results, it suffers from two drawbacks. First, the preprocessing steps may cause the optic disc boundary to become intractable because it fuses with the surrounding high intensity regions. Second, the pyramid edge detector is unable to filter noise from vessel edges adequately and active contour model will fail to outline the optic disc boundary correctly.

Similarly, while region snakes works well for optic discs with uniform intensity distribution, it tends to fail in optic discs having very low intensity or in cases where segment of optic disc has very low intensity. Application of deformable super-quadrics, or dynamic models with global and local deformation properties inherited from super-quadric ellipsoids and membrane splines, may be useful in optic disc detection. However, it will fail in cases with peripapillary atrophy, where there is a high intensity region next to the optic disc. Further, its high computational cost is not suitable for online processing of digital retinal images. These limitations motivated us to develop a robust yet efficient technique to reliably locate and outline the optic disc.

Table 1. Results for active contour models

α	β	γ	Image 1	Image 2	Image 3
0.75	1.65	0.75		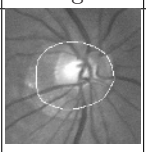	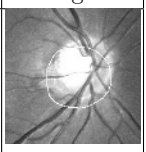
0.95	0.6	0.5		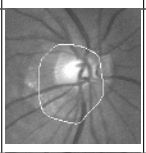	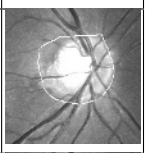
0.95	1.4	.75			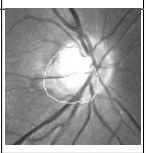
0.95	1.3	0.7			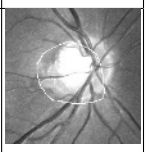
1.3	0.7	0.6		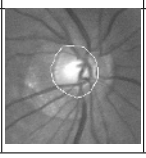	

3 Optic Disc Localization and Contour Detection

The major steps in the proposed approach to reliably detect the optic disc in large numbers of retinal images under diverse conditions are as follows. First, the approximate location of the optic disc is estimated via wavelet transform.

The intensity template is employed to construct an abstract representation of the optic disc. This abstract representation of the optic disc significantly reduces the processing area, thus increasing the computational efficiency. Next, an ellipse fitting procedure is applied to detect disc contour and to filter out difficult cases. Finally, a wavelet-based high pass filter is used to remove undesirable edge noise and to enhance the detection of non-homogenous optic discs.

Our image database consists of digital retinal images captured using a Topcon© fundus camera. All the images are standard 40-degree field of the retina centered on the macula. Image resolution is 25micron/pixel. Images were stored in 24-bit TIFF format with image size of 768*576 pixels.

3.1 Localization of Optic Disc Window by Daubechies Wavelet Transformation

Figure 2 shows the different color layers of a typical retinal image. It is evident that the optic disc outline is not present in the red layer (Fig. 2(b)) or the blue layer (Fig. 2(c)). In contrast, the green layer (Fig. 2(d)) captures the optic disc outline. We use this layer for subsequent processing.

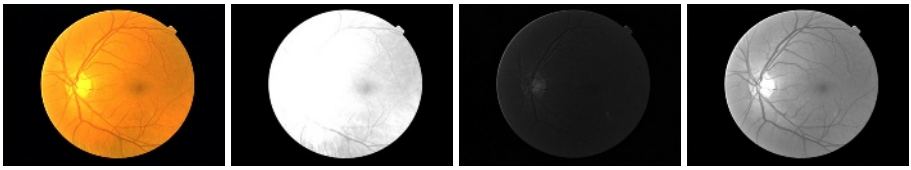

(a) Original Image (b) Red Layer (c) Blue Layer (d) Green Layer

Fig. 2. Color layers of a retinal image

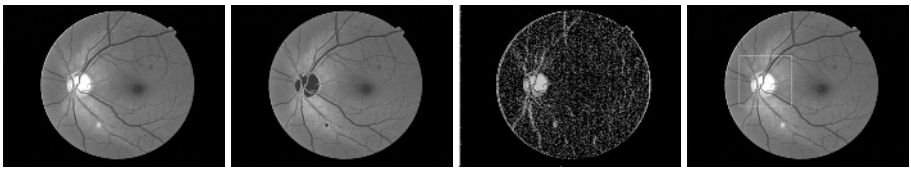

(a) (b) (c) (d)

Fig. 3. Selected optic disc region using Daubechies wavelet transform

There has been a growing interest to use wavelets as a new transform technique for image processing. The aim of wavelet transform is to 'express' an input signal as a series of coefficients of specified energy. We use the Daubechies wavelet [12] to localize the optic disc. First, a wavelet transform is carried out to obtain the wavelet coefficients. Next, an inverse wavelet transform is performed after thresholding the HH component (high pass in vertical and horizontal direction) (Fig. 3(b)). The resultant image is then subtracted from the original

retinal image to obtain the subtracted image, and its sub-images (16x16 pixels) are analyzed (Fig. 3(c)).

Note that the sub-image with the highest mean value correlates to the area inside the optic disc. Hence, the center of the sub-image ($Xc,\ Yc$) with the highest mean intensity is selected and the optic disc region is defined as a WxW window centered at ($Xc,\ Yc$). The dimension W is determined by taking into consideration the image resolution (25micron/pixel) and the average size of the optic disc in the general population. Based on the results, W is set to be 180. Fig. 3(d) shows the selected optic disc window. Experiments on 279 digital retinal images show 100% accuracy in the detection of optic disc.

3.2 Abstract Representation of Optic Disc Boundary Region

We have shown that there exist wide variations in optic disc boundary, from clear boundary outlines to very difficult cases with complex boundary outlines. To minimize the interference from these complications, we use an abstract representation of the optic to capture the optic disc boundary. This has shown to give robust results including cases with highly non-homogenous optic discs.

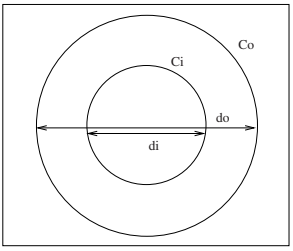

Fig. 4. Template to localize optic disc boundary

The abstract representation of the optic disc is in the form of a template is shown in Fig. 4. It consists of two circles: an inner circle C_i and an outer circle C_o. C_i denotes the approximated optic disc boundary and the region between the C_i and C_o is the immediate background. Both C_o and C_i are concentric circles, and the diameter (d_o) of C_o is defined as

$$d_o = d_i + K \tag{2}$$

The optimal K value is obtained by using a training image set. The optic disc is approximated to the template by calculating the intensity ratio (IR) as follows:

$$IR = M_i/M_o \tag{3}$$

where M_i is the mean intensity of pixels inside the circle C_i and M_o is the mean intensity of the region between circles C_i and C_o. Vessel pixels are not involved in the calculation of mean intensity to increase the accuracy. The abstract representation of the optic disc is obtained by searching for the best fitting inner circle C_i. Fig. 5 and Fig. 6 show the abstract representations obtained.

The optic disc boundary region is selected as the region between $d_i \pm K$ (Fig. 7). By processing the optic disc at an abstract level rather than pixel level, we are able to detect the optic disc boundary region accurately in cases where the optic disc is highly non-homogenous.

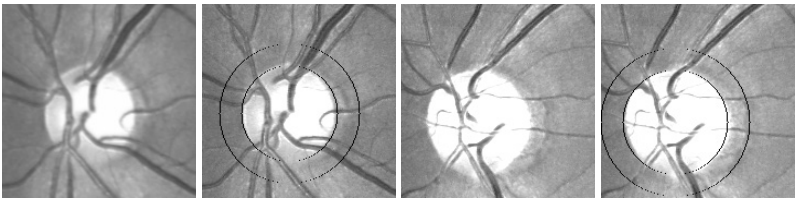

(a) (b) (c) (d)

Fig. 5. (a), (c) Uniform optic disc images; (b), (d) Fitting of template

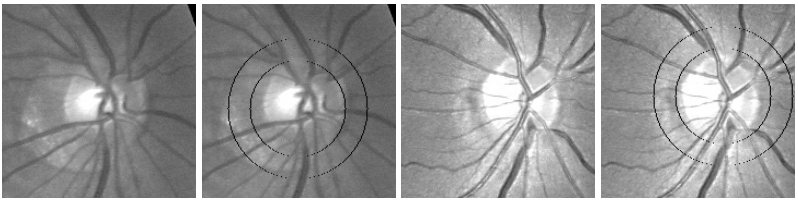

(a) (b) (c) (d)

Fig. 6. (a), (c) Non-uniform optic disc images; (b), (d) Fitting of template

3.3 Ellipse Fitting to Detect Optic Disc Contour

One of the basic tasks in pattern recognition and computer vision is the fitting of geometric primitives to a set of points. Existing ellipse fitting algorithms exploits methods such as Hough transforms [1], Kalman filtering, fuzzy clustering, or least square approach [4]. These can be divided into (1) clustering and (2) optimization based methods.

The first group of fitting techniques includes Hough transform and fuzzy clustering, which are robust against outliers and can detect multiple primitives simultaneously. Unfortunately, these techniques have low accuracy, are slow and require large amount of memory. The second group of fitting methods, which includes the Least Square approach [4], is based on the optimization of an objective function that characterizes the goodness of a particular ellipse with respect to the given set of data points. The main advantages of this group of methods

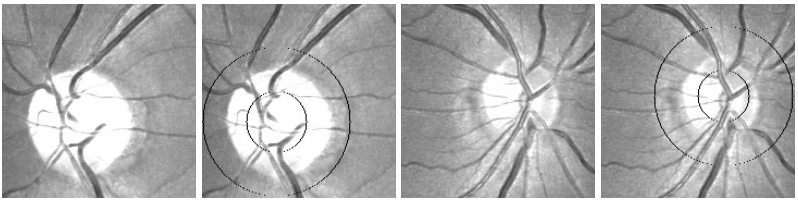

(a) (b) (c) (d)

Fig. 7. (a), (c) Optic disc regions; (b), (d) Isolated optic disc boundary region

are their speed and accuracy. However, these methods can fit only one primitive at a time, that is, the data should be pre-segmented before the fitting. Further, they are more sensitive to the effect of outlier compared to clustering methods.

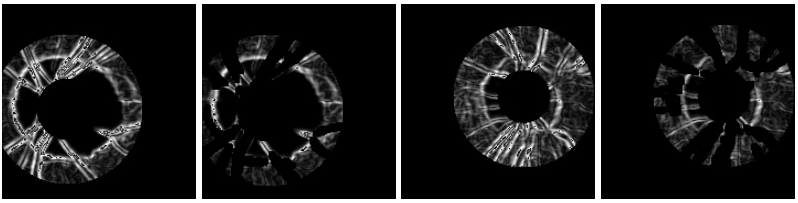

(a) (b) (c) (d)

Fig. 8. (a), (c) Sobel edge maps; (b), (d) After vessel removal

In our proposed ellipse fitting algorithm, a Sobel edge map of the optic disc boundary region is used (Fig. 8(a) and (c)). These Sobel images tend to have a high degree of noise arising from blood vessel edges and break at a number of places. Hence, we first remove all the vessel information by using a retina vessel detection algorithm [6] (Fig. 8(b) and (d)). Ellipse fitting algorithm is then used to detect optic disc contour from the resultant images.

Our ellipse fitting algorithm finds the four best fitting ellipses with minimal errors. The ellipse center is moved within the area defined by inner circle C_i. The ellipse major axis a varies between $W/2 \pm W/4$, while the minor axis b of the ellipse is restricted to $(1 \pm 0.2)*a$ pixels. These conditions are set according to the optic disc variations. The best fitting ellipses are given by

$$EF_i = P_i * (a + b) \tag{4}$$

where EF_i is the measure of ellipse fitting and P_i is the number of edge points for the ellipse i. Ellipses having four highest EF_i are selected and the intensity ratios for the four ellipses are calculated (see equation 3). The ellipse with the highest IR whose major and minor axis falls between (1 ± 0.25) d_i is regarded as the detected optic disc contour. Fig. 9 shows that the ellipse fitting procedure is able to accurately detect the optic disc boundary.

Fig. 10 depicts a difficult case where the ellipse fitting model detects part of the optic cup edge as the optic disc contour. Careful analysis reveals that this is due to the presence of optic cup edge points which tends to over-shadow the actual edge points of the optic disc boundary. In these situations, a wavelet-based enhancement is initiated.

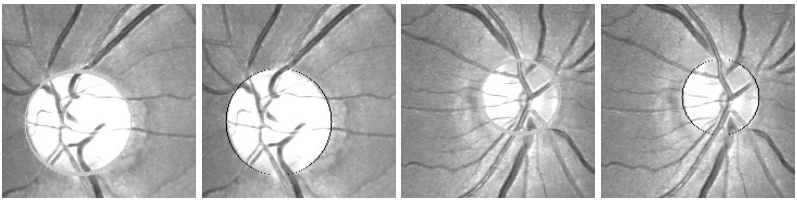

(a) (b) (c) (d)

Fig. 9. (a), (c) Four best ellipses superimposed on optic disc region; (b), (d) Correctly detected ellipse

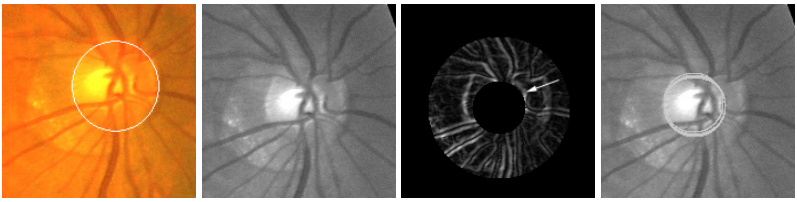

(a) (b) (c) (d)

Fig. 10. (a) Manual outline of optic disc; (b) Optic disc region green layer; (c) Arrow indicate optic cup edge interference; (d) Detected ellipses

3.4 Enhancement Using Daubechies Wavelet Transformation

To overcome the problem of noise due to the presence of optic cup points, we employ Daubechies wavelet transform [12] to enhance the optic disc boundary. This is achieved by performing the inverse wavelet transformation of coefficients after filtering out the HH component. This step gives rise to an image whose optic cup region has been removed. Fig. 11(a) shows the edge map of an inverse thresholded image. Once the edge image has been obtained, we further threshold the edge image with the image mean. This successfully removes the very prominent edge points due to optic cup and gives prominence to the faint optic disc boundary edges (Fig. 11(b)). Fig. 11(d) shows an accurately detected optic disc boundary after wavelet processing.

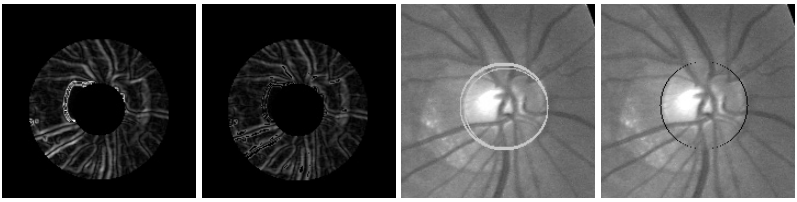

(a) (b) (c) (d)

Fig. 11. (a) Sobel edge image after wavelet enhancement; (b) Thresholding with image mean; (c) Ellipses selected by algorithm; (d) Best fitting ellipse

4 Experimental Results

We evaluated our proposed approach on 279 consecutive digital retinal images. The following performance criteria are used:

(1) *Accuracy* – Ratio of the number of acceptably detected contours as assessed by a trained medical doctor over the total number of images.

(2) *Vertical Diameter Assessment* – Average ratio of the vertical diameter of the detected contour over the vertical diameter of the actual optic disc boundary.

For criteria (2), the optic disc boundary outline of the images has been carefully traced by a trained medical doctor and the entire optic disc area is transformed to gray value of 255 with the background set to 0. The actual vertical diameter of the disc boundary is obtained from this transformed image.

Table 2 shows the results obtained. Without additional wavelet processing, the optic disc detection algorithm achieved 86% accuracy and 87% vertical diameter assessment. Using Daubechies wavelet processing to improve the difficult cases, we are able to achieve an accuracy of 94% and vertical diameter assessment of 93%. This improvement of 8% in accuracy includes the most difficult cases where the optic disc is of low intensity and is situated in a neighborhood with high intensity variations.

Table 2. Detection of optic disc contour

	Accuracy	Vertical Diameter Assessment
Ellipse fitting without wavelet processing	86% (240/279)	87%
Ellipse fitting with wavelet processing	94% (262/279)	93%

5 Discussion

Existing optic disc detection algorithms focus mainly on optic disc localization and detection of the optic disc boundary. Optic disc localization is important as it reduces the computational cost. [8] propose an optic disc localization algorithm using pyramidal decomposition. Potential optic disc regions are located using Haar wavelet-based pyramidal decomposition and are analyzed using Hausdorff template matching to detect probable optic disc. [18] design a localization algorithm based on variance of image intensity. The variance of intensity of adjacent pixels is used for recognition of the optic disc. The original retinal image is subdivided into sub-images and their respective mean intensities are calculated. Variance image is formed by a transformation which include mean of the sub-image. The location of the maximum of this image is taken as the centre of the optic disc.

[13] employs clustering techniques with simple thresholding to select several probable optic disc regions. These regions are clustered into groups and further analyzed by principle component analysis to identify the optic disc. This algorithm has yielded robust results in images with large high intensity lesions such as hard exudates in diabetic retinopathy. The drawbacks are that they are time-consuming and the results are not easily reproducible [24].

Optic disc contour detection has been attempted with active contour models [10,16] and template matching [8]. Active contour models have failed to detect optic disc contour accurately due to the presence of noise, various lesions, intensity changes close to retinal vessels, and other factors. Various preprocessing techniques have been employed to overcome these problems, including morphological filtering, pyramid edge detection, etc., but no large scale testing has been carried out to validate their accuracies. In this work, we have compared the proposed algorithm with active contour models to validate its robustness. Template matching [8] yields better results because it tends to view the optic disc as a whole entity rather than processing at pixel level. However, none of the algorithms has been tested on a large number of images and proven to be sufficiently robust and accurate for clinical use.

6 Conclusion

In this paper, we have presented an optic disc detection algorithm that employs ellipse fitting and wavelet processing to detect optic disc contour accurately. Experimental results have shown that the algorithm is capable of achieving 94% accuracy for the optic disc detection and 93% accuracy for the assessment of vertical optic disc diameter in 279 consecutive digital retinal images obtained from patients in a diabetic retinopathy screening program. The assessment of vertical optic disc diameter, when combined with parameters such as the vertical optic cup diameter, can provide useful information for the diagnosis and follow up management of glaucoma patients.

References

1. Aguado, A.S., Nixon, M.S.: A New Hough Transform Mapping for Ellipse Detection. Technical Report, University of Southampton (1995)
2. Balo, K.P., Mihluedo, H., Djagnikpo, P.A., Akpandja, M.S., Bechetoille, A.: Correlation between Neuroretinal Rim and Optic Disc Areas in Normal Melanoderm and Glaucoma Patients. J Fr Ophtalmol. 23 (2000)
3. Bonomi, L., Orzalesi, N.: Glaucoma: Concepts in Evolution. Morphometric and Functional Parameters in the Diagnosis and Management of Glaucoma. Kugler Publications, New York (1991)
4. Fitzgibbon, A., Pilu, M., Fisher, R.B.: Direct Least Square Fitting of Ellipses. IEEE Tran. on Pattern Analysis & Machine Intelligence 21 (1999)
5. Hamilton, A.M.P., Ulbig, M.W., Polkinghorne, P.: Management of Diabetic Retinopathy. (1996)
6. Hsu, W., Pallawala, P.M.D.S., Lee, M.L., Au-Eong, K.G.: The Role of Domain Knowledge in the Detection of Retinal Hard Exudates. IEEE Conf. on Computer Vision and Pattern Recognition (2001)
7. Kass, A., Witkin, A., Terzopoulos, D.: Snakes: Active contour models. Int. Journal of Computer Vision (1988)
8. Lalonde, M., Beaulieu, M., Gagnon, L.: Fast and Robust Optic Disc Detection Using Pyramidal Decomposition and Hausdorff-Based Template Matching. IEEE Trans. on Medical Imaging (2001)
9. Larsen, H.W.: Manual and Color Atlas of the Ocular Fundus (1976)
10. Lee, S., Brady, M.: Optic Disc Boundary Detection. British Machine Vision Conference (1989)
11. Leroy, B., Herlin, I.L., Cohen, L.D.: Multi-Resolution Algorithms for Active Contour Models, Int. Conf. on Analysis and Optimization of Systems (1996)
12. Lewis, A., Knowles, G.: Image Compression Using the 2-D Wavelet. IEEE Trans. on Image Processing (1992)
13. Li, H., Chutatape, O., Automatic Location of Optic Disc in Retinal Images. Int. Conf. on Image Processing (2001)
14. Mendels, F., Heneghan, C., Harper, P.D., Reilly, R.B., Thiran, J-P.: Extraction of the Optic Disc Boundary in Digital Fundus Images. First Joint BMES/EMBS Conf. Serving Humanity, Advancing Technology (1999)
15. Mendels, F., Heneghan, C., Thiran, J-P.: Identification of the Optic Disc Boundary in Retinal Images Using Active Contours. Irish Machine Vision and Image Processing Conf. (1999)
16. Morris, D.T., Donnison, C.: Identifying the Neuro-Retinal Rim Boundary Using Dynamic Contours. Image and Vision Computing 17 (1999)
17. Park, H.W., Schoepflin, T., Kim, Y.: Active Contour Model with Gradient Directional Information: Directional Snake. IEEE Trans. On Circuits and Systems for Video Technology (2001)
18. Sinthanayothin, C., Boyce, J.F., Cook, H.L., Williamson, T.H.: Automated Localization of Optic Disc, Fovea and Retinal Blood Vessels from Digital Color Fundus Images. British Journal of Ophthalmology(1999)
19. Wang, H., Hsu, W., Goh, K.G., Lee, M.L.: An Effective Approach to Detect Lesions in Color Retinal Images. IEEE Conf. on Computer Vision and Pattern Recognition (2000)
20. World Health Organization Fact Sheet No. 138 (2002)

21. Xu, C., Prince, J.L.: Generalized Gradient Vector Flow External Forces for Active Contours. Signal Processing (1998)
22. Xu, C., Prince, J.L.: Snakes, Shapes, and Gradient Vector Flow. IEEE Trans. on Image Processing (1988)
23. Xu, C., Yezzi, A., Prince, J.L.: On the Relationship Between Parametric and Geometric Active Contours. 34th Asimolar Conf. on Signals, Systems, and Computers (2000)
24. Yogesan, K., Barry, C.J., Jitskaia, L., Eikelboom, Morgan, W.H., House, P.H., Saarloos, P.P.V.: Software for 3-D Visualization/Analysis of Optic-Disc Images. IEEE Engineering in Medicine and Biology (1999)